Supplementary Information

Theoretical Insights into the Generation and Reactivity of Hydride on ZnO($10\bar{1}0$) Surface

Xian-Yang Zhang,[a] Zhi-Qiang Wang,[*a] and Xue-Qing Gong[*b]

[a]State Key Laboratory of Green Chemical Engineering and Industrial Catalysis, Centre for Computational Chemistry and Research Institute of Industrial Catalysis, School of Chemistry and Molecular Engineering, East China University of Science and Technology, 130 Meilong Road, Shanghai, 200237, China.

[b]School of Chemistry and Chemical Engineering, Shanghai Jiao Tong University, 800 Dongchuan Road, Shanghai, 200240, China.

Corresponding authors: zhiqiangwang@ecust.edu.cn, xqgong@sjtu.edu.cn

Supplementary Figures and Tables

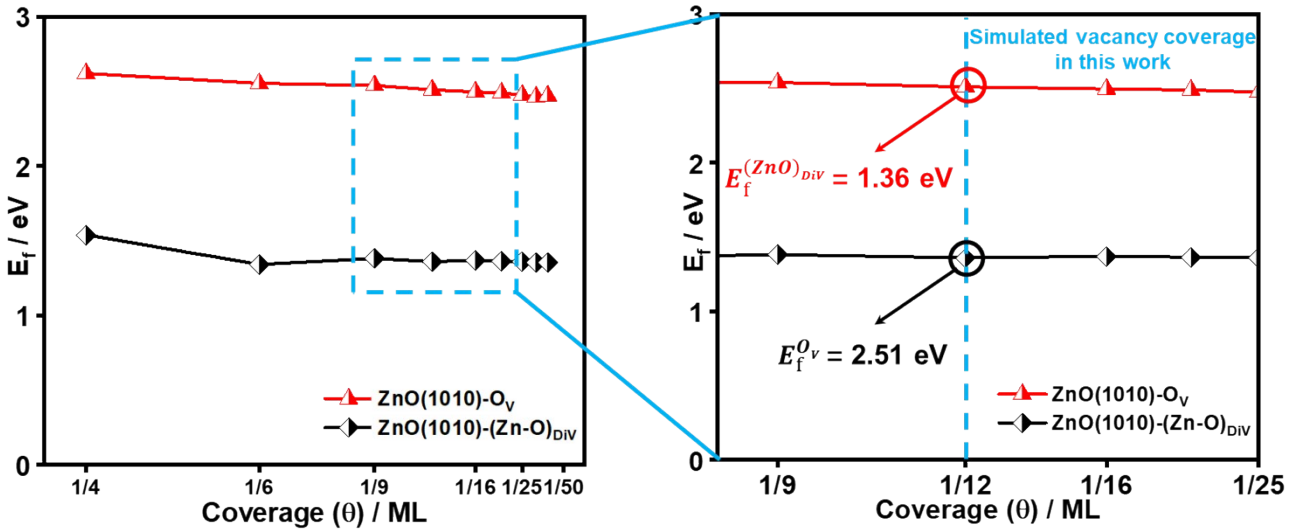

Fig. S1. Calculated formation energies (E_f) as a function of vacancy coverage (θ) / ML for oxygen vacancy (O_V) and Zn-O dimer vacancies ($(Zn\text{-}O)_{DiV}$) on the ZnO($10\bar{1}0$) surface.

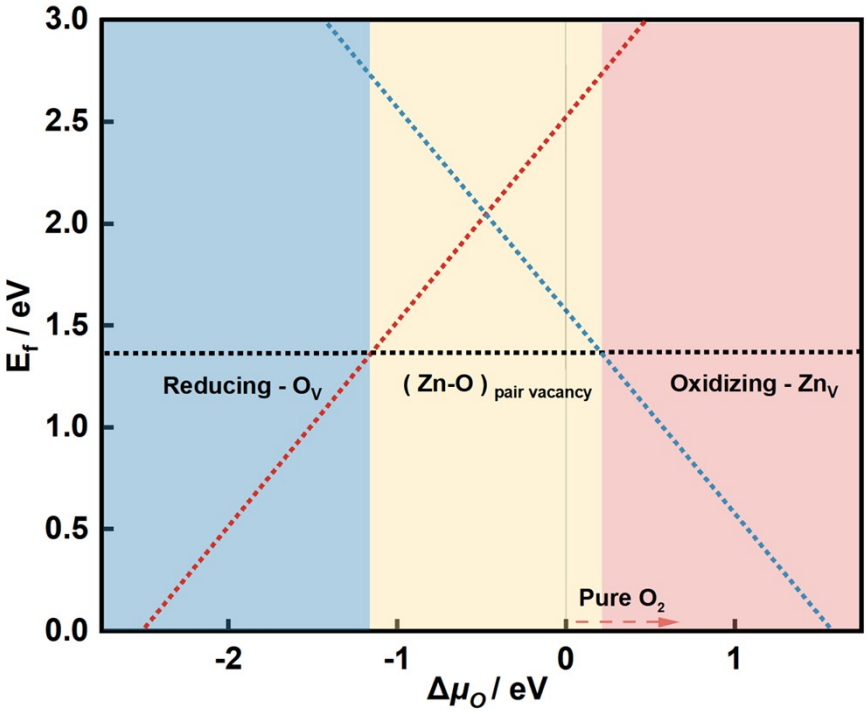

Fig. S2. Calculated relationship between the formation energies (E_f) of different defect ZnO surfaces and chemical potentials of oxygen ($\Delta\mu_O$).

To obtain the chemical potentials of oxygen under certain conditions and evaluate the stabilities of the different defect ZnO($10\bar{1}0$) surfaces, one can also align the surface energetics with other types of reaction gases. As an example, we can refer to the balanced reaction below:

$$CO_2 = CO + ½O_2 \#(S1)$$

For Equation S1, the balance constant can be expressed as:

$$K_p = \frac{p_{CO} \cdot (p_{O_2})^{\frac{1}{2}}}{p_{CO_2}} \#(S2)$$

where p_{CO}, p_{O_2} and p_{CO_2} represent the balanced partial pressure of CO, O_2 and CO_2 molecules, respectively. Therefore, the chemical potential of O_2 has an alternative expression:

$$\Delta\mu_{O_2} = RTln\frac{p_{O_2}}{p^\theta} = RTln\frac{(\frac{K_p \cdot p_{CO_2}}{p_{CO}})^2}{p^\theta} = 2RT\left(lnK_p + ln\frac{p_{CO_2}}{p_{CO}}\right) \#(S3)$$

where the p^θ is the standard pressure (1 bar = 101.325 kPa). Notably, the K_p can be also determined by:

$$K_p = \exp\left(-\frac{\Delta G}{RT}\right) \#(S4)$$

where ΔG represents the Gibbs free energy change of the reaction. To determine the Gibbs free energies of the reactants, Shomate equation can be used, for which the parameters (A, B, C, D, E) are obtained by NIST Chemistry Book[1]:

$$C_p^\circ(T) = A + Bt + Ct^2 + Dt^3 + \frac{E}{t^2} \#(S5)$$

where $C_p^\circ(T)$ represents the thermal capacity of a substance under certain temperature. With Shomate equation, the entropy, enthalpy, and Gibbs free energy can be obtained with:

$$H^\circ(T) = H^\circ(298.15\ K) + \int_{298.15}^{T} C_p^\circ(T)dT \#(S6)$$

$$S^\circ(T) = S^\circ(298.15\ K) + \int_{298.15}^{T} \frac{C_p^\circ(T)}{T}dT \#(S7)$$

$$G^\circ(T) = H^\circ(T) - TS^\circ(T) \#(S8)$$

In addition, the boundary line between Zn_V and $(Zn\text{-}O)_{DiV}$ phase follows the relationship of (p_{CO2}/p_{CO})-T solved under $\Delta\mu_{O_2}$= 0.44 eV (namely $\Delta\mu_O$= 0.22 eV), and the boundary line between $(Zn\text{-}O)_{DiV}$ and O_V phase

follows the relationship of (p_{CO2}/p_{CO})-T solved under $\Delta\mu_{O_2}$= -2.30 eV (namely $\Delta\mu_O$= -1.15 eV). The values of $\Delta\mu_O$ are determined by the two intersection points in Figure S2.

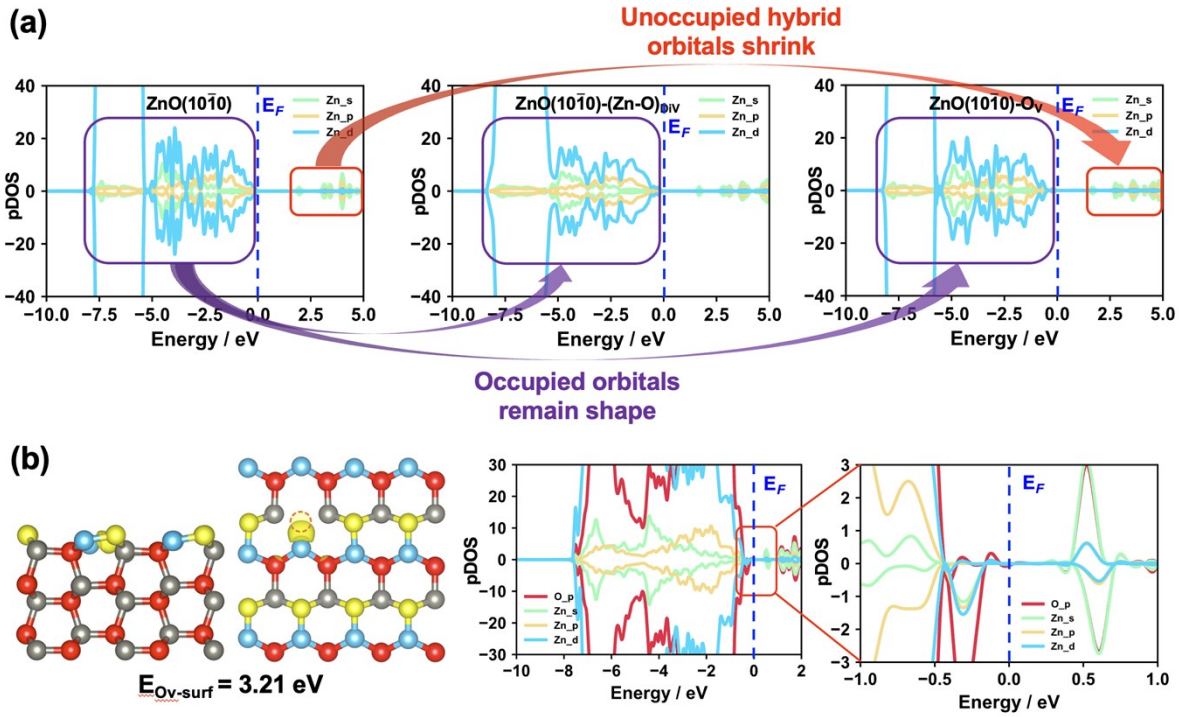

Fig. S3. (a) Calculated partial density of states (pDOS) of Zn atoms on various defect ZnO($10\bar{1}0$) surfaces. (b) Calculated oxygen vacancy formation energy and spin charge density differences (left: side view, right: top view) and pDOS of O_V surface, for which the excess electrons are localized at oxygen vacancy site. The form of *dsp* hybrid orbitals for the excess electrons are illustrated. Sky blue and red spheres represent surface Zn and surface O atoms, grey and yellow spheres represent subsurface Zn and subsurface O atoms, while dot lines of red represent O vacancies, respectively. Red, green, yellow and sky blue lines represent O(*p*), Zn(*s*), Zn(*p*), and Zn(*d*) DOS, respectively. These notations are used throughout the paper.

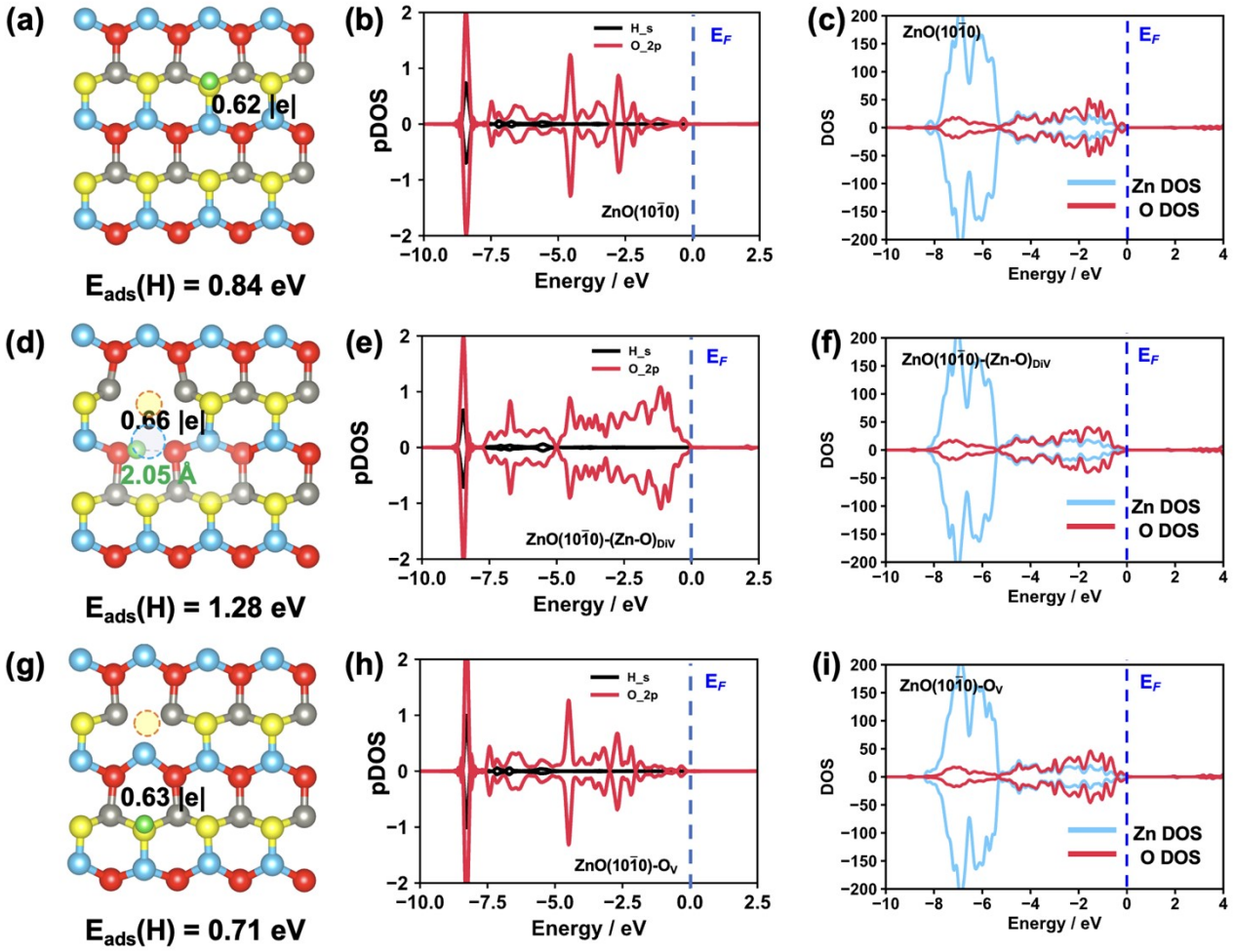

Fig. S4. Calculated structures and density of states of the O-H species on various ZnO($10\bar{1}0$) surfaces with one H being adsorbed at O sites. (a, d, g) Calculated structures (top view) and adsorption energies of single H adsorbed at O atoms of different ZnO($10\bar{1}0$) surfaces ((a) pristine (d) $(Zn\text{-}O)_{DiV}$ (g) O_V). Green: H atoms. The corresponding Bader charge values of the H atoms are also shown. (b, c, e, f, h, i) Calculated partial density of states (pDOS) of single H adsorbed at O of different ZnO systems ((b, c) pristine, (e, f) $(Zn\text{-}O)_{DiV}$ and (h, i) O_V surfaces). Black and red lines represent H(1*s*) and O(2*p*) pDOS, respectively. The Fermi energy level (E_F) are marked as blue dashed lines, and all DOS are aligned with respect to the E_F. These notations are used throughout the paper.

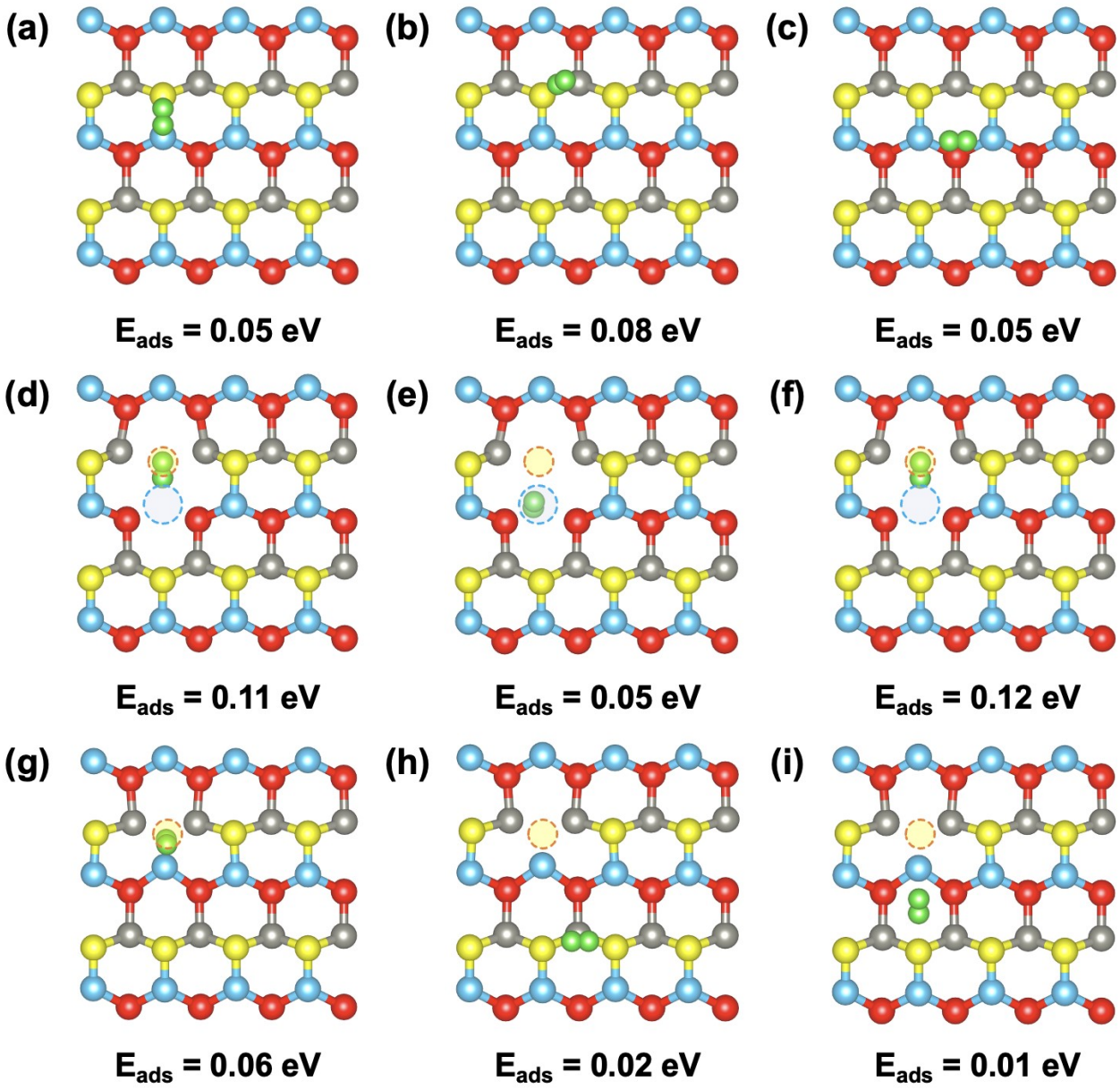

Fig. S5. Calculated structures (top view) and adsorption energies of H_2 at different sites of pristine and various defect ZnO($10\bar{1}0$) surfaces. (a-c), (d-f) and (g-i) represent H_2 adsorbed on pristine ZnO($10\bar{1}0$), $(Zn\text{-}O)_{DiV}$ and O_V surfaces. (a), (d) and (g) represent the adsorption sites for heterolytic H_2 dissociation. (b), (e) and (h) represent the double O adsorption sites for homolytic H_2 dissociation and 2 O-H species formation. (c), (f) and (i) represent the double Zn adsorption sites for homolytic H_2 dissociation and 2 Zn-H species formation.

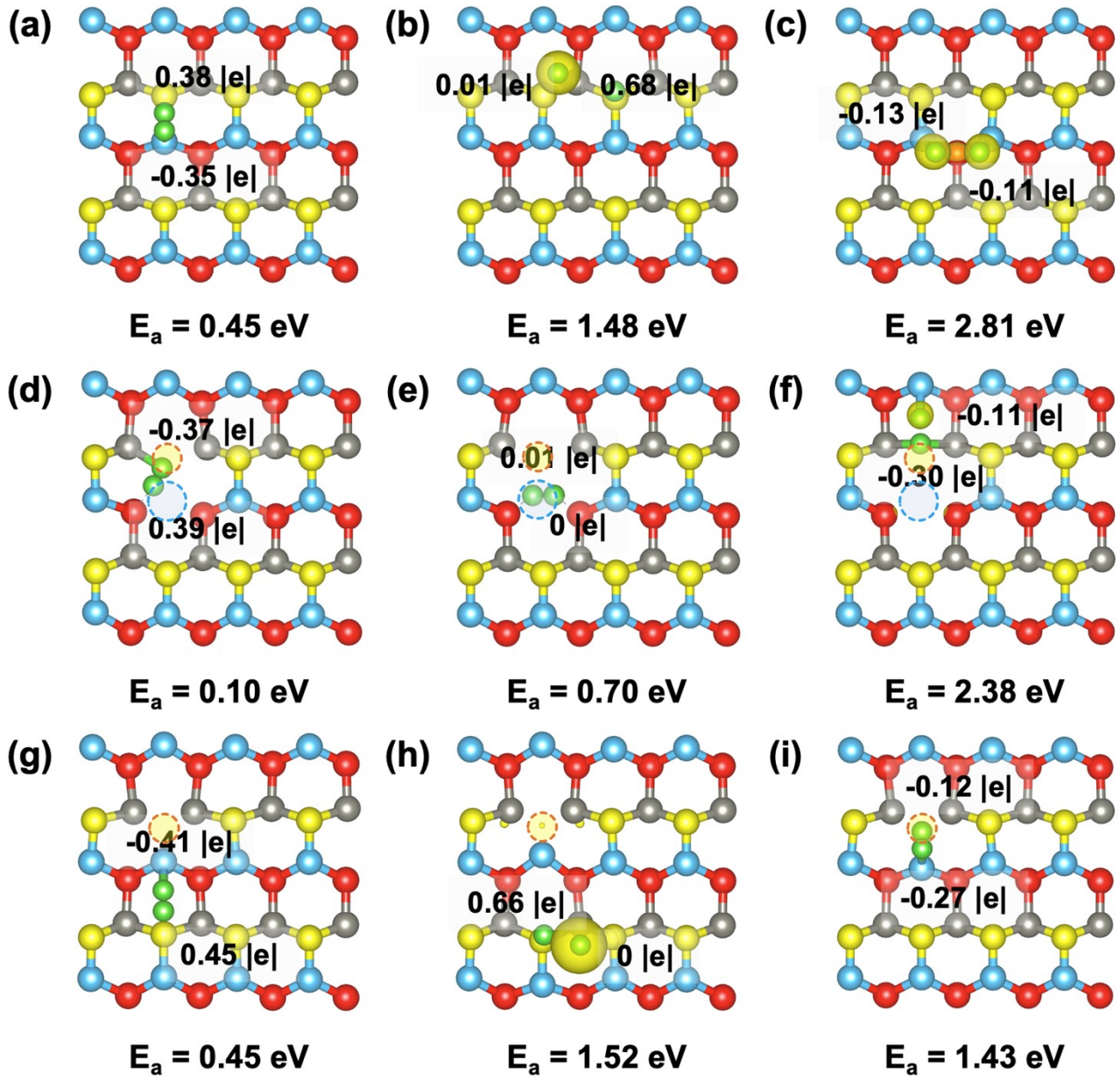

Fig. S6. Calculated transition state (TS) structures (top view) and energy barriers of H_2 dissociation on different ZnO($10\bar{1}0$) surfaces. The calculated Bader charge values are also shown. (a-c), (d-f) and (g-i) represent the transition states of heterolytic H_2 dissociation on the pristine, $(Zn\text{-}O)_{DiV}$ and O_V surfaces. (a), (d) and (g) represent the adsorption sites for heterolytic H_2 dissociation. (b), (e) and (h) represent homolytic H_2 dissociation, forming 2 O-H species. (c), (f) and (i) represent the double Zn adsorption sites for homolytic H_2 dissociation and 2 Zn-H species formation. The spin iso-surfaces (yellow) are plotted at a value of 0.05 e/Å^3, and the corresponding Bader charge values of the H atoms are also shown.

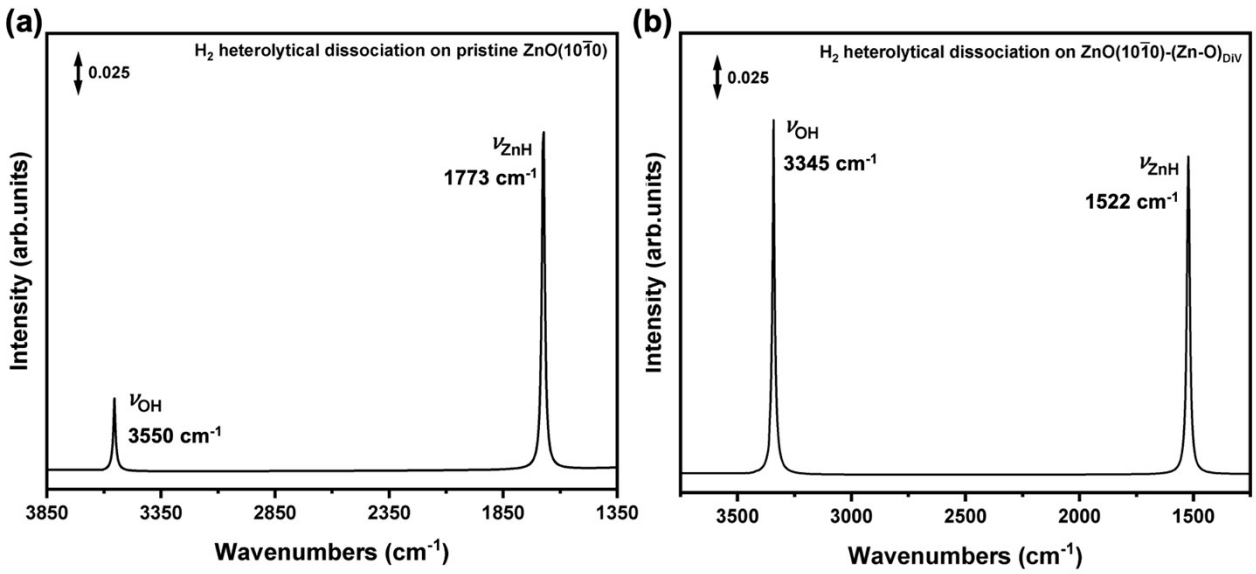

Fig. S7. Calculated infrared (IR) spectrum of (a) pristine ZnO$(10\bar{1}0)$ and (b) ZnO$(10\bar{1}0)$-$(Zn\text{-}O)_{DiV}$ surfaces containing dissociated H_2. The ν_{OH} and ν_{ZnH} represent the stretching vibrations of the O-H and Zn-H bonds, respectively.

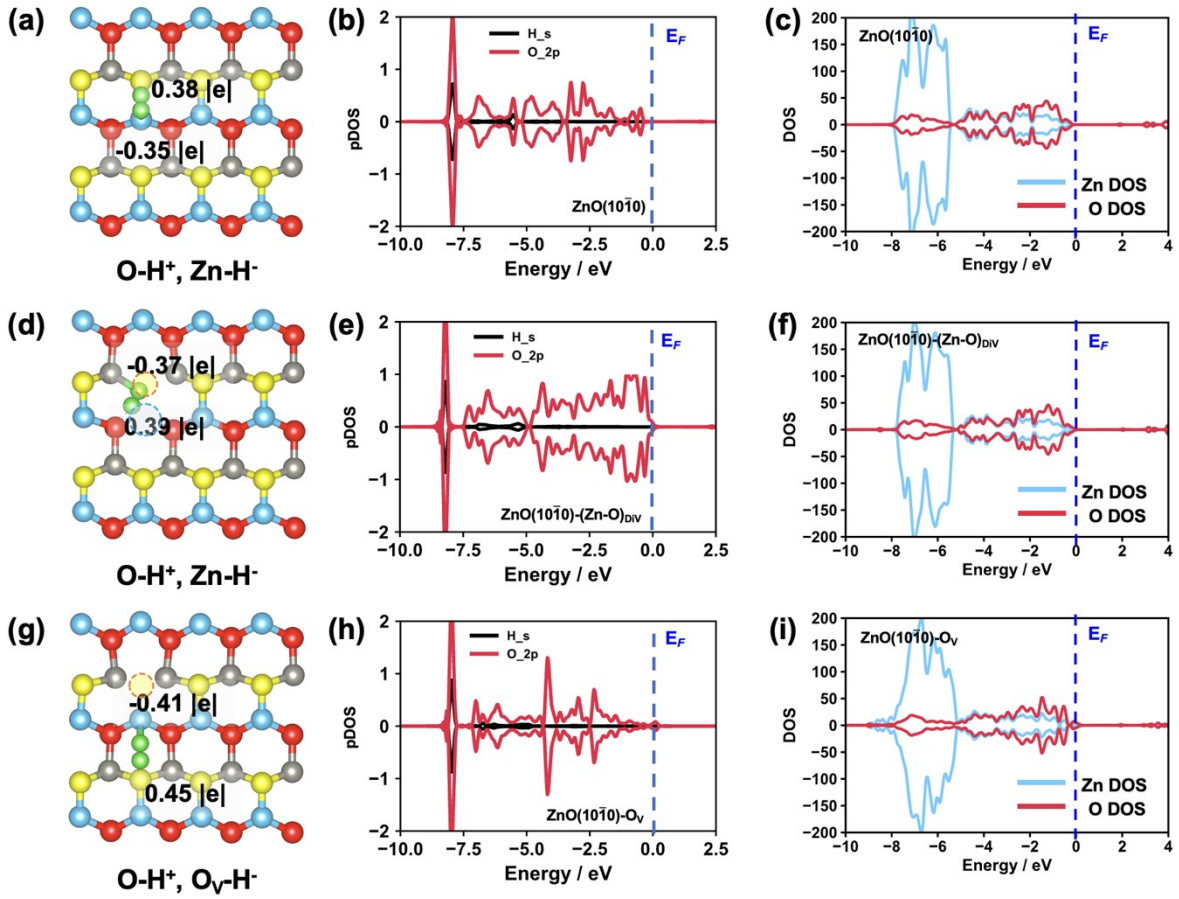

Fig. S8. Calculated structures (top view) and DOS of heterolytic H_2 dissociation on different ZnO($10\bar{1}0$) surfaces. (a) pristine, (d) $(Zn\text{-}O)_{DiV}$, and (g) O_V surfaces. The corresponding Bader charge values of the H atoms are also shown. (b, e, h) Calculated partial density of states of O and H species in these ZnO systems ((b) clean, (e) $(Zn\text{-}O)_{DiV}$ and (h) O_V surfaces/subsurface). (c, f, i) Calculated density of states of heterolytic H_2 dissociation on different ZnO($10\bar{1}0$) surfaces. ((c) pristine, (f) $(Zn\text{-}O)_{DiV}$ and (i) O_V surfaces). E_F are marked as blue dashed lines, and all DOS are aligned with respect to the E_F.

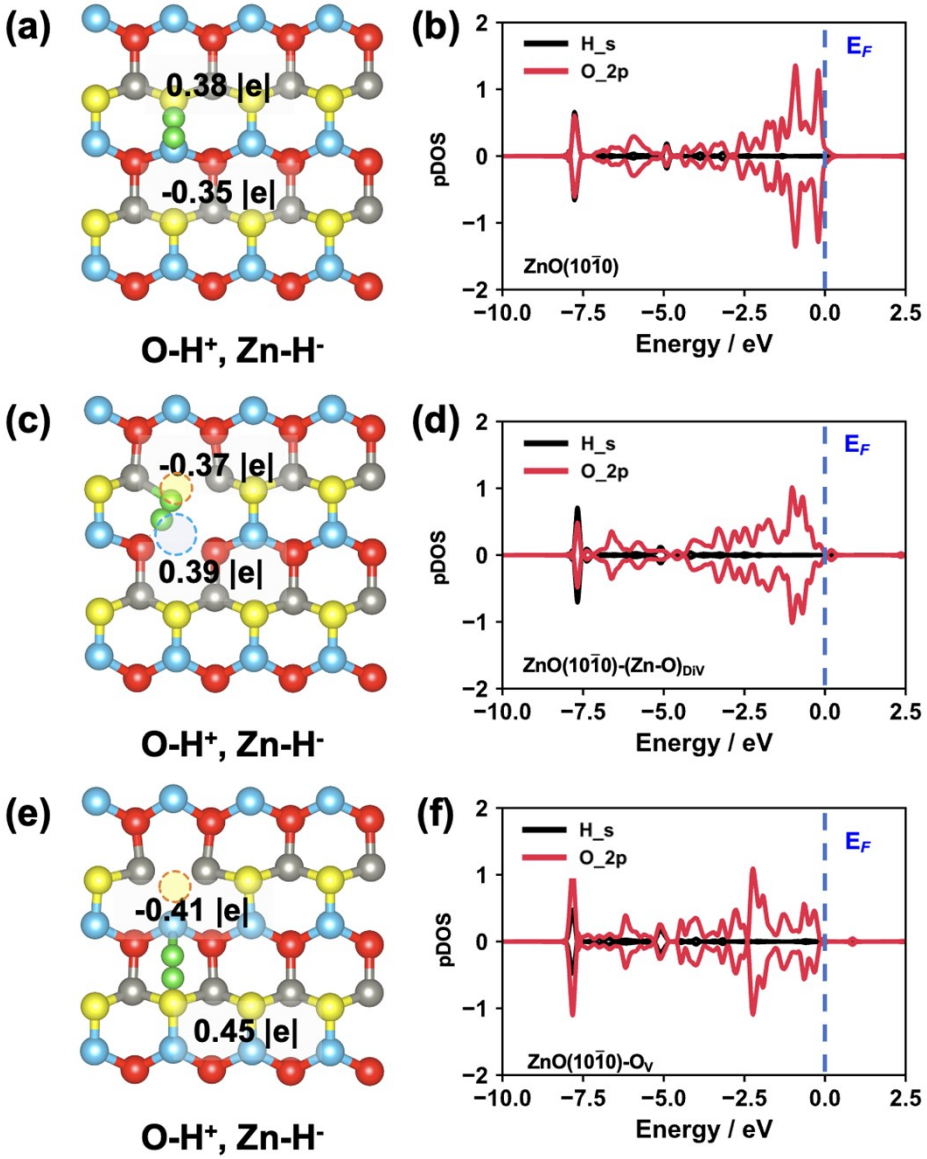

Fig. S9. Calculated TS structures (top view) of the of heterolytic H_2 dissociation on different ZnO($10\bar{1}0$) surfaces. (a) pristine, (c) $(Zn\text{-}O)_{DiV}$ and (e) O_V surfaces. The corresponding Bader charge values of the H atoms are also shown. (b, d, f) Calculated partial density of states (pDOS) of O and H in these ZnO systems ((b) pristine, (d) $(Zn\text{-}O)_{DiV}$ and (f) O_V surfaces). Black and red lines represent H(1*s*) and O(2*p*) pDOS, respectively. E_F are marked as blue dashed lines, and all DOS are aligned with respect to the E_F.

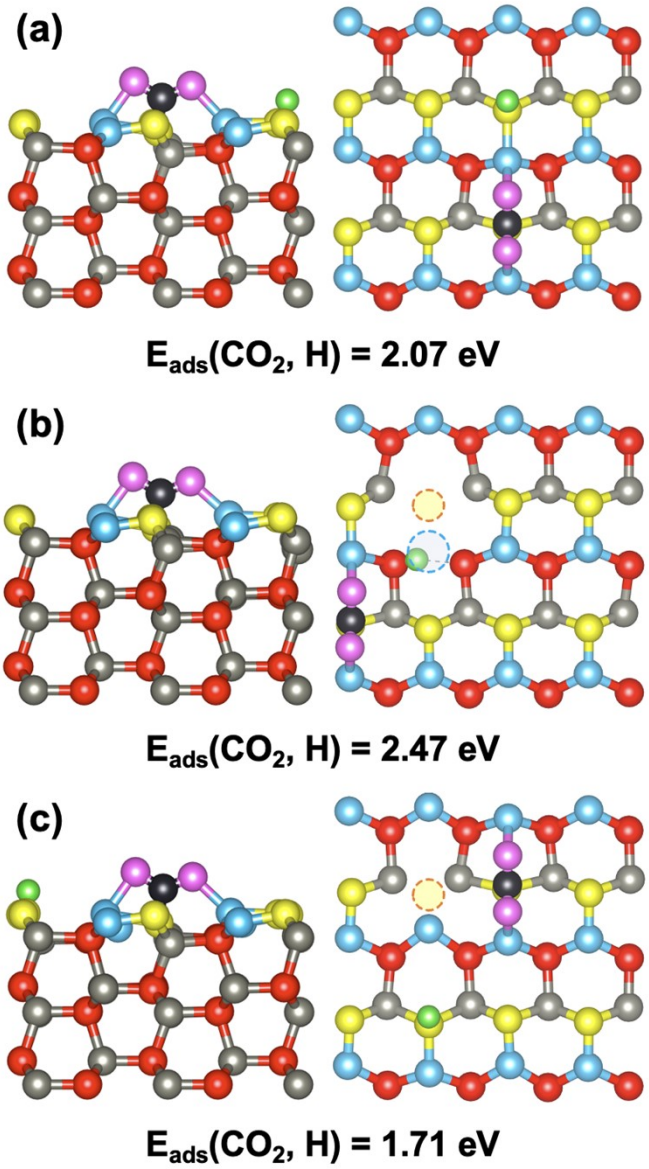

Fig. S10. Calculated structures (left: side view, right: top view) and adsorption energies of one H co-adsorbed with CO_2 on different ZnO($10\bar{1}0$) surfaces. (a) pristine, (b) $(Zn\text{-}O)_{DiV}$ and (c) O_V surfaces. Pink and black balls represent O_{CO2} and C atoms, respectively. This notation is used throughout the paper.

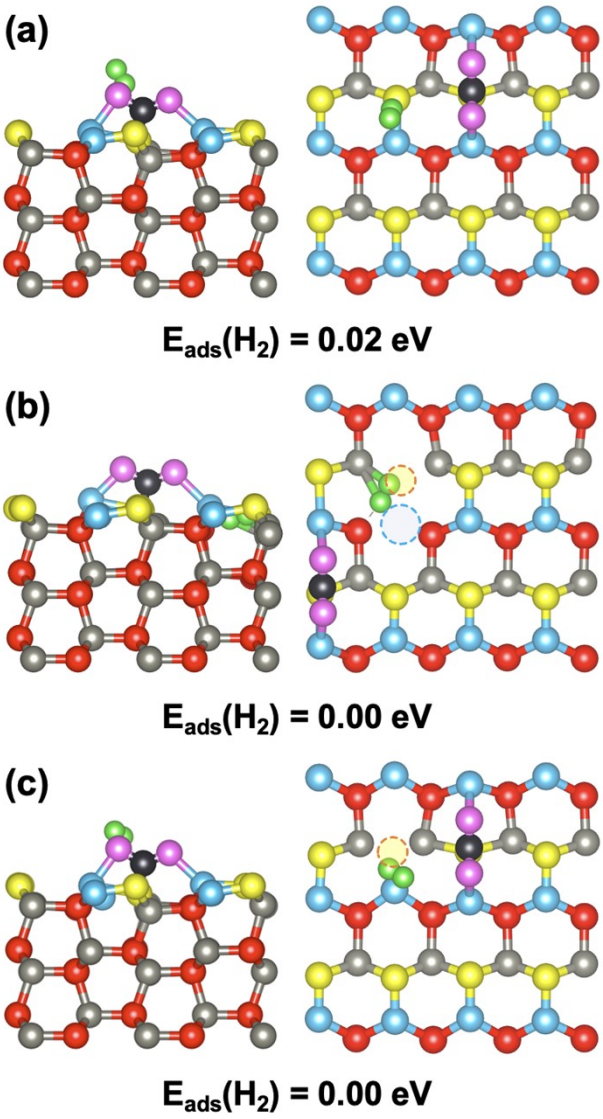

Fig. S11. Calculated structures (left: side view, right: top view) and adsorption energy of H_2 with adsorbed CO_2 on different ZnO($10\bar{1}0$) surfaces. (a) pristine, (b) $(Zn\text{-}O)_{DiV}$ and (c) O_V surfaces.

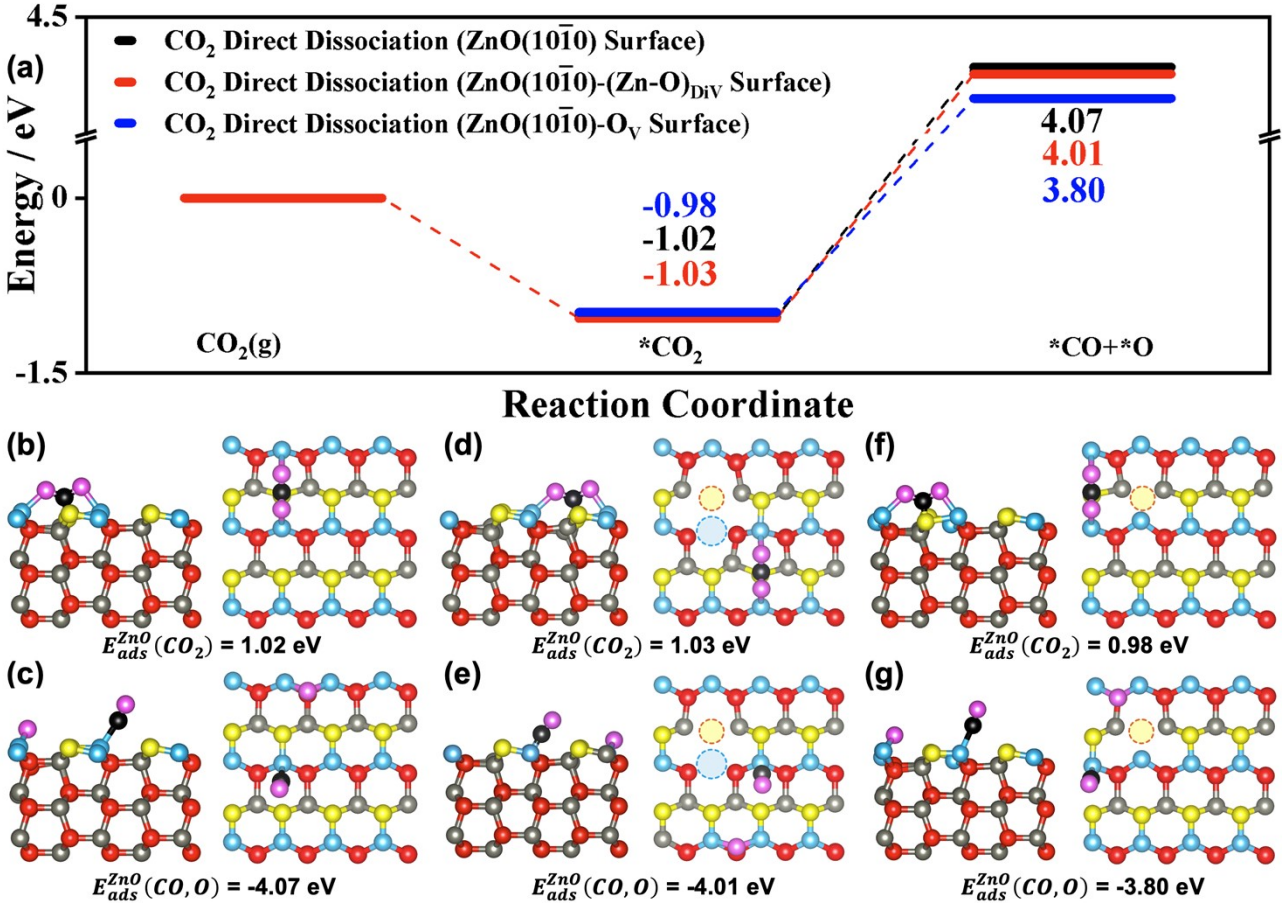

Fig. S12. (a) Calculated energy profile of direct CO_2 dissociation on the pristine and defect ZnO($10\bar{1}0$) surface. (b-g) Calculated structures (left: side view, right: top view) and adsorption energies of CO_2 adsorption (b, d, f) and dissociation products (c, e, g) on (b, c) pristine, (d, e) $(Zn\text{-}O)_{DiV}$ and (f, g) O_V surfaces.

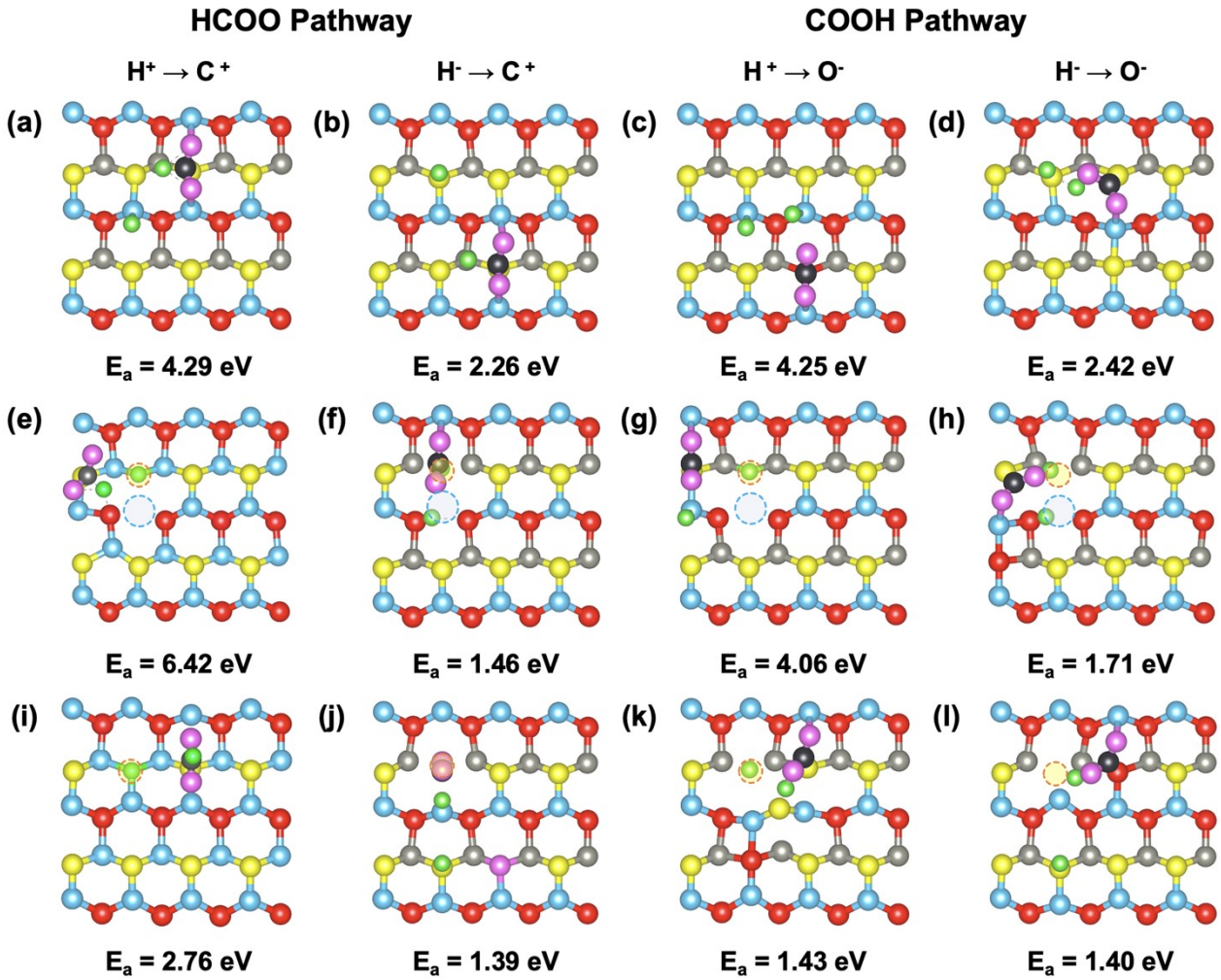

Fig. S13. Calculated TS structures (top view) and energy barriers of CO_2 hydrogenation on different ZnO($10\bar{1}0$) surfaces. (a-d) pristine, (e-h) $(Zn\text{-}O)_{DiV}$ and (i-l) O_V surfaces. Route of HCOO is divided into different attribute of active H (*i.e.*, H^+ ((a), (e) and (i)) and H^- ((b), (f) and (j)) species), so as the route of COOH (*i.e.*, H^+ ((c), (g) and (k)) and H^- ((d), (h) and (l)) species).

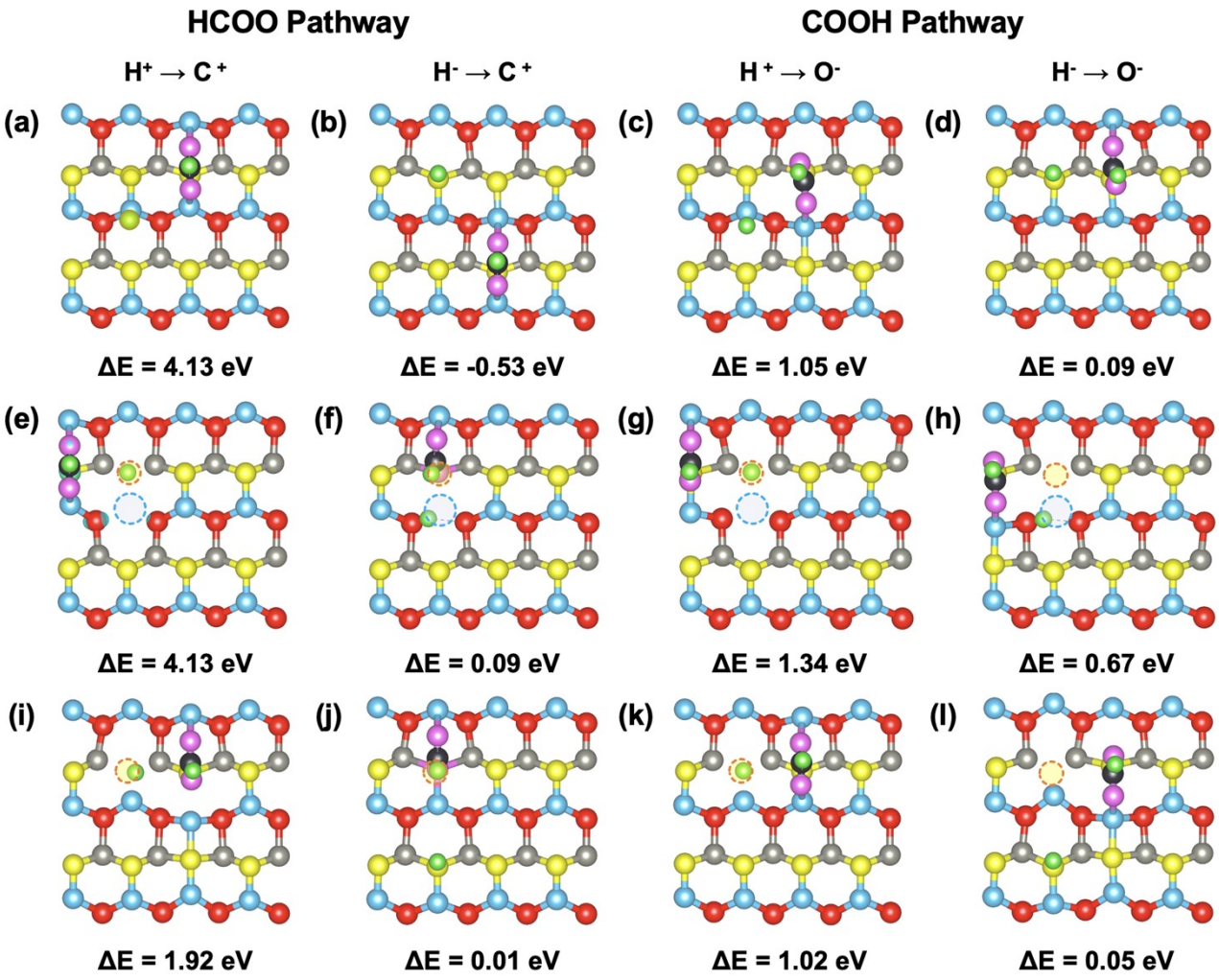

Fig. S14. Calculated HCOO/COOH structures (top view) and corresponding reaction energy (ΔE) of CO_2 hydrogenation on different ZnO($10\bar{1}0$) surfaces. (a-d) pristine, (e-h) $(ZnO)_{DiV}$ and (i-l) O_V surfaces. Route of HCOO is divided according to the different kinds of active H (*i.e.*, H^+ and H^- species), so as the route of COOH.

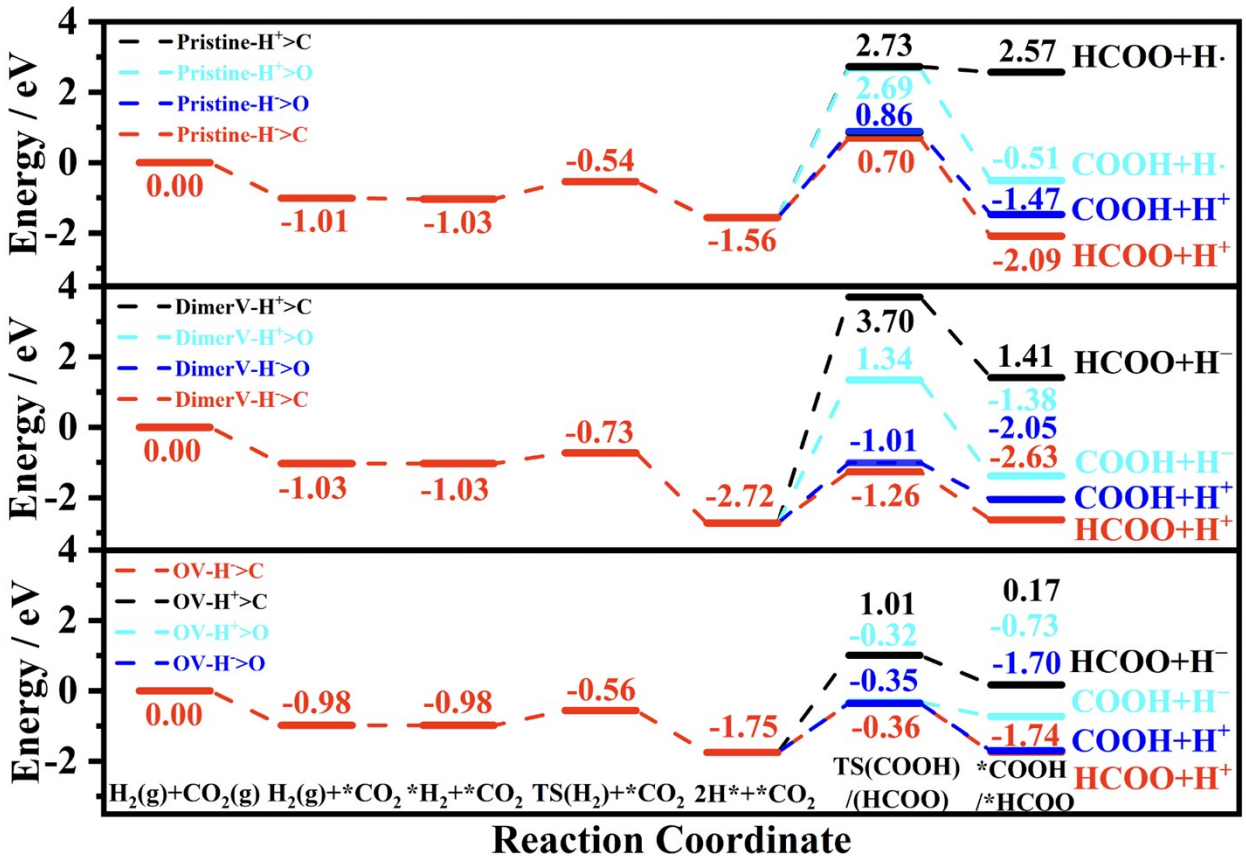

Fig. S15. Calculated energy profiles of CO_2 hydrogenation on three different ZnO($10\bar{1}0$) surfaces. Black, cyan, blue and red lines represent routes with final products of HCOO + H^-, COOH + H^-, COOH + H^+ and HCOO + H^+ species, respectively.

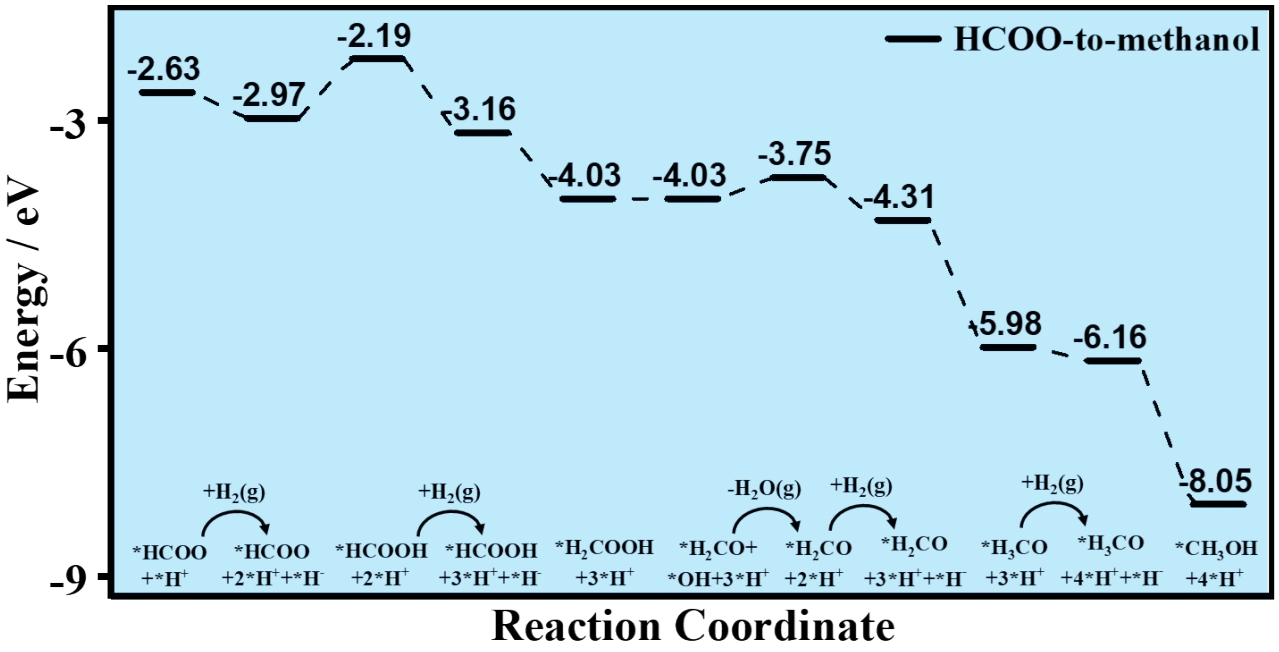

Fig. S16. Calculated energy profile of the HCOO-to-methanol pathway (following the co-adsorption of *HCOO and *H species) of CO_2 hydrogenation on the ZnO($10\bar{1}0$)-$(Zn\text{-}O)_{DiV}$ surface.

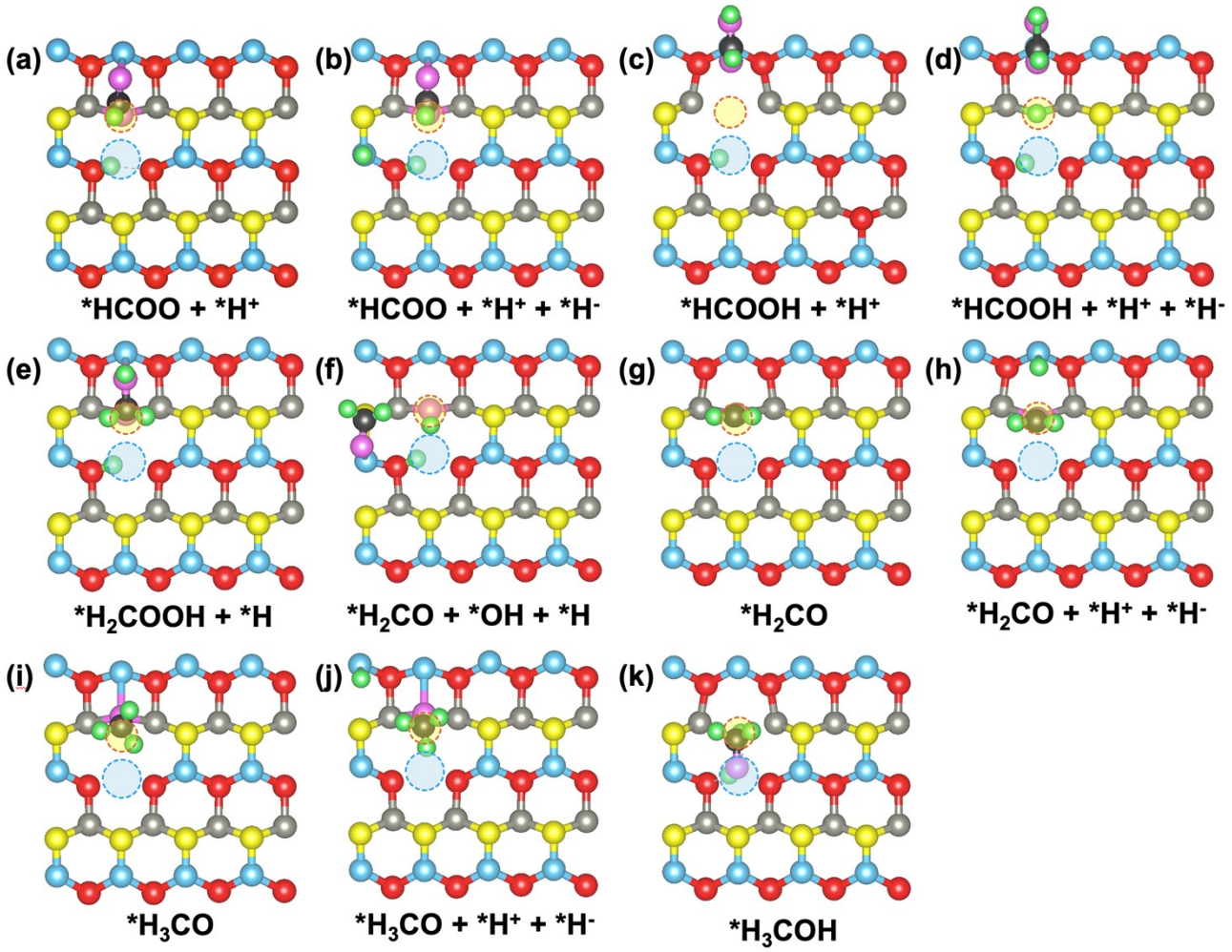

Fig. S17. Calculated structures (top view) of key intermediates during CO_2 hydrogenation in the HCOO-to-methanol pathway (starting from the co-adsorption of *HCOO and $*H^+$ species) on the ZnO($10\bar{1}0$)-$(Zn\text{-}O)_{DiV}$ surface.

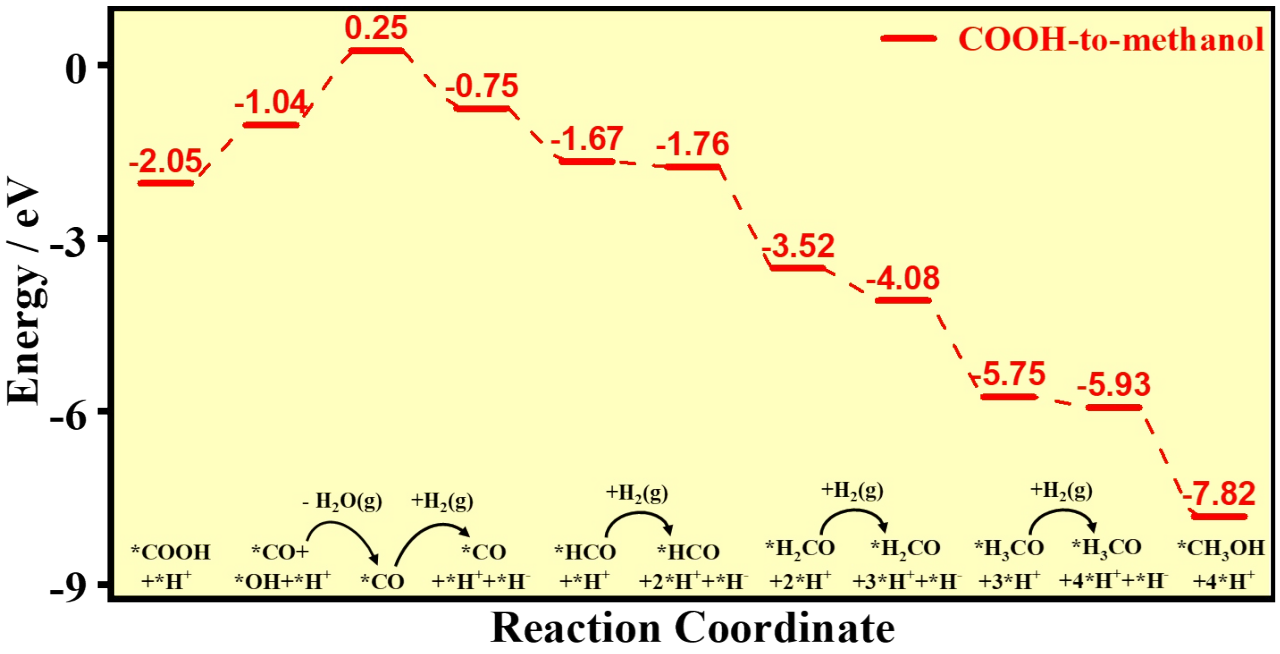

Fig. S18. Calculated energy profile of the COOH-to-methanol pathway (following the co-adsorption of *COOH and *H species) of CO_2 hydrogenation on the ZnO($10\bar{1}0$)-$(Zn\text{-}O)_{DiV}$ surface.

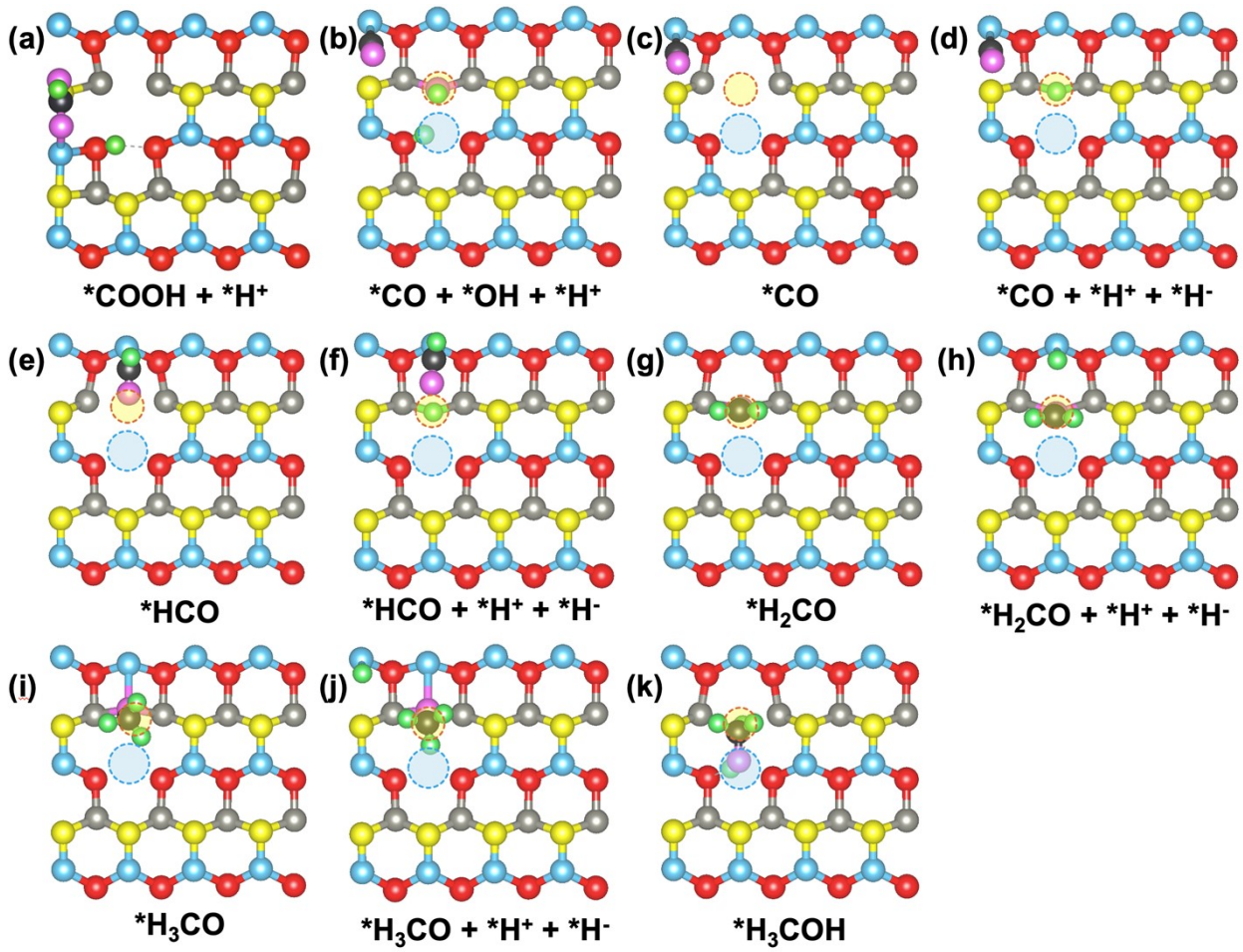

Fig. S19. Calculated structures (top view) of key intermediates during CO_2 hydrogenation in the COOH-to-methanol pathway (starting from the co-adsorption of *COOH and $*H^+$ species) on the ZnO($10\bar{1}0$)-$(Zn\text{-}O)_{DiV}$ surface.

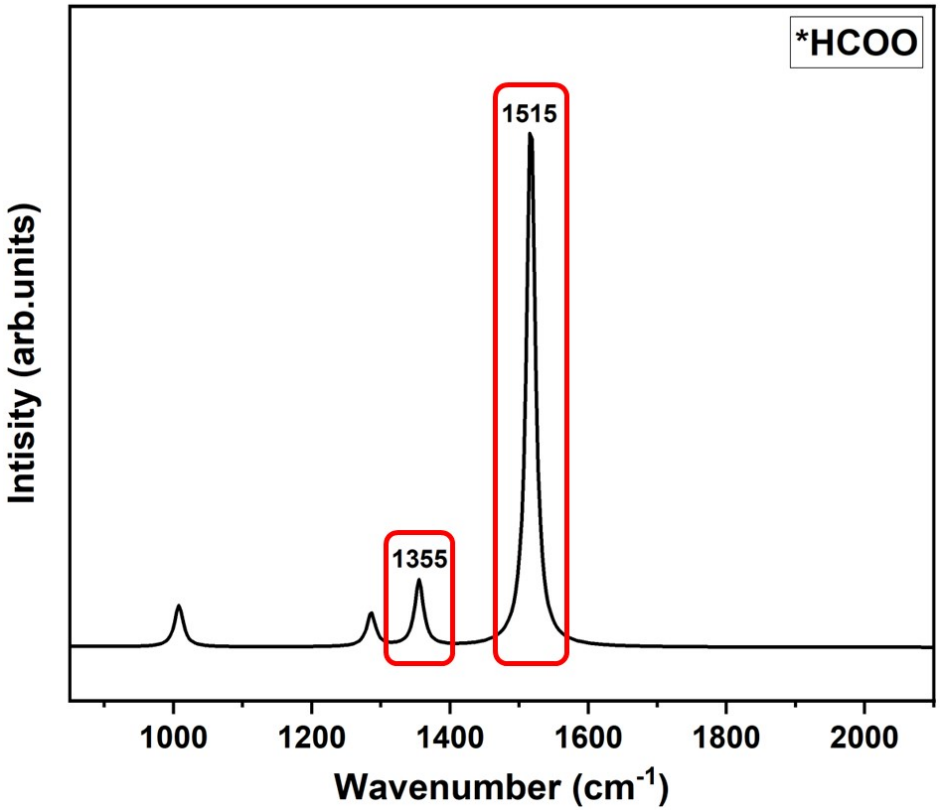

Fig. S20. DFPT calculated IR spectrum of HCOO species adsorbed on pristine ZnO($10\bar{1}0$) surface.

To validate the calculation methods, especially for the charges of atoms, we have systematically tested a series of charge models on different defect ZnO($10\bar{1}0$) surfaces, *i.e.*, Bader charge model[2–5], Charge Model 5 (CM5) and Hirschfield charge model[6–11]. The calculated results are shown in Table S1. Code of the density derived electrostatic and chemical (DDEC) method and corresponding manual were obtained at: https://github.com/berquist/chargemol. Bader charge v1.04, was obtained at: https://theory.cm.utexas.edu/henkelman/code/bader/.

Table S1. Calculated net charge value of single adsorbed H and heterolytically dissociated H_2 on pristine and different defect ZnO($10\bar{1}0$) surfaces with Bader, CM5 and Hirschfield charge models.

			Bader / |e|	CM5 / |e|	Hirschfield / |e|
Single H	Pristine	H^+	0.62	0.49	0.33
		H•	-0.16	-0.02	-0.03
	DiV	H^+	0.63	0.46	0.29
		H^-	-0.40	-0.08	-0.09
	O_V	H^+	0.66	0.48	0.32
		H^-	-0.42	-0.06	-0.08
H_2 Heterolytic Dissociation	Pristine	H^+	0.66	0.47	0.31
		H^-	-0.40	-0.16	-0.17
	DiV	H^+	0.69	0.48	0.33
		H^-	-0.38	-0.06	-0.08
	O_V	H^+	0.75	0.46	0.30
		H^-	-0.42	-0.09	-0.10

Table S2. Calculated Bader charges of heterolytically dissociated H_2 and accumulated Bader charges of corresponding ZnO layers of pristine and various defects ZnO($10\bar{1}0$) surfaces. The surface Zn-O layer is denoted as Layer 1, the middle Zn-O layer is denoted as Layer 2, and the bottom Zn-O layer is denoted as Layer 3.

System	Clean surface / |e|	$(Zn\text{-}O)_{DiV}$ Surface / |e|	O_V Surface / |e|
2 adsorbed H	0.26	0.30	0.34
Layer 1	-0.13	-0.58	-0.57
Layer 2	-0.09	0.25	-0.45
Layer 3	-0.05	0.02	-0.59

References

1 P. J. Linstrom and W. G. Mallard, NIST Standard Reference Database Number 69, eds. National Institute of Standards and Technology, Gaithersburg MD, 20899, retrieved April 13, 2024.

2 W. Tang, E. Sanville and G. Henkelman, *J. Phys. Condens. Matter*, 2009, **21**, 084204.

3 E. Sanville, S. D. Kenny, R. Smith and G. Henkelman, *J. Comput. Chem.*, 2007, **28**, 899–908.

4 G. Henkelman, A. Arnaldsson and H. Jónsson, *Comput. Mater. Sci.*, 2006, **36**, 354–360.

5 M. Yu and D. R. Trinkle, *J. Chem. Phys.*, 2011, **134**, 064111.

6 T. A. Manz, *RSC Adv.*, 2017, **7**, 45552–45581.

7 T. A. Manz and N. G. Limas, *RSC Adv.*, 2016, **6**, 47771–47801.

8 N. G. Limas and T. A. Manz, *RSC Adv.*, 2016, **6**, 45727–45747.

9 T. A. Manz and D. S. Sholl, *J. Chem. Theory Comput.*, 2012, **8**, 2844–2867.

10 T. A. Manz and D. S. Sholl, *J. Chem. Theory Comput.*, 2010, **6**, 2455–2468.

11 T. A. Manz and D. S. Sholl, *J. Chem. Theory Comput.*, 2011, **7**, 4146–4164.